DOI: 10.1002/ejic.201001011

Radicals of Free and Zinc(II)-Coordinated α-Azophenols

Amélie Kochem,[a] Maylis Orio,[b] Christian Philouze,[a] Hélène Jamet,[b] Amaury du Moulinet d'Hardemare,*[a] and Fabrice Thomas*[a]

Keywords: N ligands / Zinc / Radicals / Hydrazones / Redox chemistry

The tridentate 2-*tert*-butyl-4-methoxy-6-(quinolin-8-ylazo)-phenol ligand HL has been synthesized and structurally characterized. Its redox activity has been investigated by electrochemical measurements and DFT calculations. Oxidation of HL (irreversible process) affords primarily a hydrogen-bonded phenoxyl radical, whereas its reduction affords an iminosemiquinonate radical species. The reaction of two equivalents of HL with $Zn(OAc)_2$ affords the zinc complex $Zn(L)_2$, which has been structurally characterized. Its oxidation is easier than that of HL and is reversible. The EPR spectrum of $[Zn(L)(L^{\cdot})]^+$ shows an unresolved ($S = 1/2$) signal at $g = 2.005$, while $[Zn(L^{\cdot})]^{2+}$ exhibits spin triplet resonances ($|D| = 0.0118\ cm^{-1}$ and $E/D = 0$). The extra delocalization of spin density on the azo group contributes to a lowering of the D value relative to those of Schiff base derivatives. The temperature dependence of the EPR signal and DFT calculations reveal an excited state for the spin triplet and a weak exchange coupling constant $J = -2.73\ cm^{-1}$.

Introduction

A number of proteins are believed to use free radicals, which are generated on their own peptide chain, to assist redox processes occurring during turnovers.[1] Galactose oxidase (GO) is a nonheminic radical metalloenzyme that catalyzes the oxidation of primary alcohols to aldehydes.[2] The most salient feature in its active site is the direct coordination of a tyrosyl radical to the copper(II) ion. The high efficiency of the enzyme, combined with the fact that the co-oxidant is molecular dioxygen, makes GO a target for the design of new catalysts operating under mild conditions. In this context, we and other teams have developed several biomimetic complexes involving a coordinated phenoxyl radical,[3] especially from Schiff bases.[4] In a different approach, Xiang et al. have described the synthesis of a bis-(hydrazone) complex by aerobic oxidation of the copper(II) complex of (1-pyridin-2-yl-ethylidene)hydrazine under basic conditions in the presence of alcohol. A radical mechanism reminiscent of the one operated by GO for alcohol oxidation was proposed by the authors to account for ring closure, although no hydrazyl intermediate could be trapped.[5] We therefore thought it interesting to synthesize new phenol ligands that incorporate a coordinating azo (or hydrazone, see below) group and investigate their redox activity. We report in this paper the synthesis of the tridentate 2-*tert*-butyl-4-methoxy-6-(quinolin-8-ylazo)phenol ligand HL, which is derived from the prototypical tridentate Schiff base HL_{SB} (Scheme 1).[6–8] The spectroscopic, structural, and electrochemical properties of the free ligand and its zinc(II) complex are described herein.

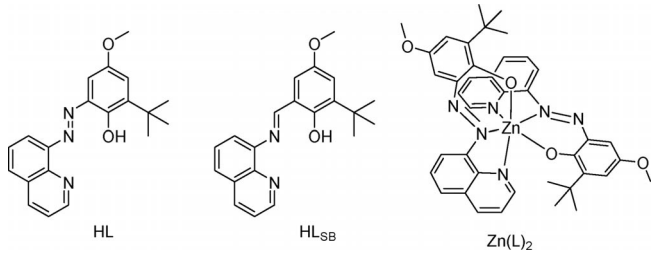

Scheme 1. Ligands and complexes of interest in this study.

Results and Discussion

The intensely colored HL[9] was obtained in good yield by coupling azotized 8-aminoquinoline with 2-*tert*-butyl-4-methoxy-phenol. The X-ray crystal structure of HL (Figure 1) shows that the two aromatic rings are strictly coplanar. The short O1–N1 distance [2.539(8) Å] evidences a strong intramolecular hydrogen bond in HL. It must be emphasized that HL may exist on either the azo/phenolate ("OH") or hydrazone/quinone ("NH") tautomeric forms (Scheme 2).[10] The short C1–O1 bond length [1.260(6) Å] indicates that the tautomeric equilibrium is displaced towards the "NH" form in the solid state.[11] DFT calculations performed on HL ("NH" and "OH" forms) confirm

[a] Département de Chimie Moléculaire, Chimie Inorganique Redox Biomimétique (CIRE), UMR-5250, Université Joseph Fourier,
BP 53, 38041 Grenoble Cedex 9, France
Fax: +33-476 51 4836
E-mail: Fabrice.Thomas@ujf-grenoble.fr
[b] Département de Chimie Moléculaire, Chimie Théorique, UMR-5250, Université JosephFourier,
BP 53, 38041 Grenoble Cedex 9, France
Supporting information for this article is available on the WWW under http://dx.doi.org/10.1002/ejic.201001011.

that the "NH" form is more stable.[12] Nevertheless, it should be pointed out that the calculated energy difference is only 3.0 kcal/mol, suggesting that the "OH" form may also be relevant (Figure 2). The cyclic voltammetry (CV) curve of HL in CH_2Cl_2 (see Supporting Information) displays two irreversible oxidation waves at +0.52 and +0.76 V vs. Fc/Fc^+, as well as a poorly reversible one-electron reduction wave at $E_{1/2}$ = –1.55 V. The irreversibility of the oxidation waves precludes characterization of the oxidized species by experimental methods. The electronic structure of the monocation has thus been investigated solely by DFT calculations. Similarly to HL, two tautomeric forms, "NH" and "OH", were considered for $(HL^{\cdot})^+$. The former was found to be more stable by 8.3 kcal/mol, definitely ruling out the existence of the "OH" tautomer cation. Only the relevant "NH" form will therefore be described. Positive spin populations are found at the O1 (0.16), C2 and C6 (0.10, 0.11), C4 (0.15), and O2 (0.10) atoms, that is, the resonant positions for the phenoxyl radicals. Non-negligible spin population is also found on the N1 (0.16), C14 (0.10), and C12 atoms (0.11), suggesting that significant delocalization occurs on the quinoline group.

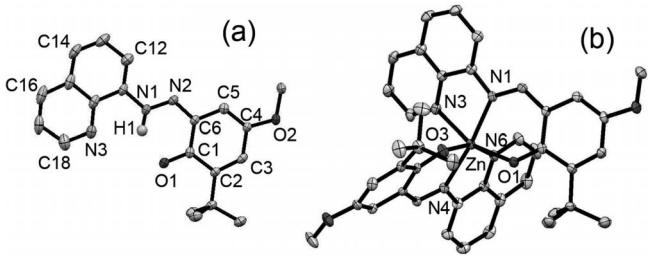

Figure 1. X-ray crystal structures of HL (a) and $Zn(L)_2$ (b) shown with 30% thermal ellipsoids. Selected bond lengths [Å] and angles [°]: (a) C1–O1 1.260(6), C4–O2 1.357(6), C6–N2 1.331(7), N1–N2 1.302(6), O1–N1 2.539(8), O1–H1–N1 134.6. (b) Zn–O1 2.032(3), Zn–O3 2.018(3), Zn–N1 2.116(3), Zn–N3 2.190(3), Zn–N4 2.137(3), Zn–N6 2.162(3), O3–Zn–N6 159.1(1), O1–Zn–N3 159.4(1), N1–Zn–N4 171.1(1).

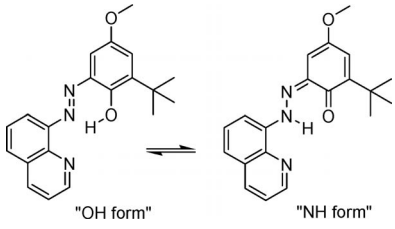

Scheme 2. Tautomeric equilibrium of HL.

Regarding the reduction process, a qualitative spectroelectrochemical investigation could be performed in addition to DFT calculations, since the redox system is not fully irreversible ($I_{p,c}/I_{p,a}$ = 20). Upon reduction, the intense band at 535 nm characteristic of HL[9] is slightly redshifted, whereas a shoulder appears at approximately 650 nm. Such absorptions have been previously reported for semiquinonate radicals.[3] DFT calculations on $(HL^{\cdot})^-$ reveal that the energy difference between the "NH" and "OH" forms is

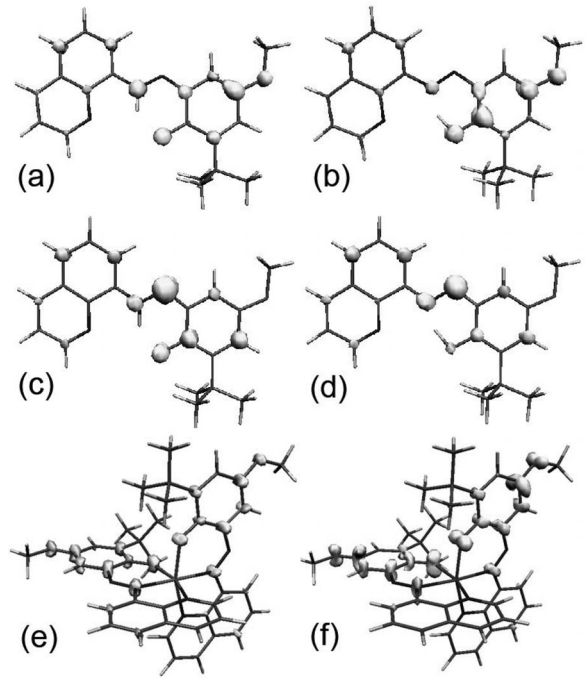

Figure 2. Spin-density plots for $(HL^{\cdot})^+$: (a) "NH form", (b) "OH form". Spin-density plots for $(HL^{\cdot})^-$: (c) "NH form", (d) "OH form". Spin-density plots for (e) $[Zn(L)(L^{\cdot})]^+$ and (f) $[Zn(L^{\cdot})_2]^{2+}$. For the atom labeling in the organic part, see Figure 1 (a). The detailed individual contributions are given in the Supporting Information.

rather small (3.4 kcal/mol), the former species being the more stable. The spin-density plot shows significant spin population at the C1, C3, C5, O1, N1, and N2 atoms and, to a lesser extent, at the C12 and C14 atoms of the quinoline group. The anion thus exhibits a mixed hydrazyl–iminosemiquinonate (highly delocalized) radical character, with delocalization on the quinoline. One can observe that the individual contributions of the N1, N2, and O1 atoms are slightly different in the "NH" and "OH" forms (0.06, 0.31, 0.12, and 0.13, 0.27, 0.05, respectively), evidencing a more marked hydrazyl radical character when the proton is located at the oxygen.

The zinc–phenolate complex $Zn(L)_2$ was obtained by reacting $Zn(OAc)_2$ with two equivalents of HL in MeOH, in the presence of NEt_3. It is almost isostructural (Figure 1) with the previously reported $Zn(L_{SB})_2$.[7] The zinc(II) ion lies within an octahedral geometry, coordinated in a meridional fashion by two deprotonated ligands, with a *cis* orientation of the phenolate moieties. Interestingly, the pyridine and phenolate rings are more twisted in $Zn(L)_2$ (21.4° and 23.8° in the two ligand moieties) than in $Zn(L_{SB})_2$. The CV curve of $Zn(L)_2$ is characterized by two reversible one-electron oxidation waves at $E_{1/2}^1$ = +0.16 V and $E_{1/2}^2$ = +0.41 V vs. Fc/Fc^+. They correspond to the successive oxidation of the phenolate moieties into phenoxyl radicals. The reduction of $Zn(L)_2$ is irreversible and occurs at the low $E_{p,c}$ value of –1.92 V. This has therefore not been further investigated. The X-band EPR spectrum of the electrogenerated monocation in CH_2Cl_2 displays an unresolved (S = 1/2) sig-

nal centered at g = 2.005 (peak-to-peak line width of 5 G), confirming its radical nature. The UV/Vis spectrum of the so-called $[Zn(L)(L^{\cdot})]^+$ species is less intense than that of $Zn(L)_2$,[9] with additional bands at 425 nm and 605 nm, where the phenoxyl π–π* transitions are expected to be found (see Supporting Information).[3] The structural changes resulting from monoradical formation have been investigated by DFT calculations: A significant elongation of the Zn–O and Zn–N_{azo} bonds (by 0.02 and 0.015 Å respectively) as well as an elongation, albeit to a lesser extent, of the C–O bonds are observed, in agreement with the radical character of the ring. The Zn–$N_{quinoline}$ bond is shortened by approximately 0.04 Å, showing that the metal–ligand interaction is strengthened at the *trans* position of the phenoxyl oxygen. In agreement with the bond length analysis, positive spin populations are found at the O1 (0.12), C2,6 (0.07), C4 (0.11) and O5 (0.05) (phenoxyl ring), and N1 (0.08) atoms. Interestingly, the spin density is found to be equally shared between the two ligand moieties. $[Zn(L)(L^{\cdot})]^+$ is found to be poorly stable in solution at room temperature (> 99% decomposition after 10 min at 298 K), in contrast to $[Zn(L_{SB})(L_{SB}^{\cdot})]^+$, for which no significant decomposition was observed after 15 h at 298 K.[7] The chemical instability of $[Zn(L)(L^{\cdot})]^+$ could be correlated to its higher oxidation potential {$E_{1/2}^1$ = +0.16 vs. $E_{1/2}^1$ = –0.02 V for $[Zn(L_{SB})_2]$}. The 100 K X-band EPR spectrum recorded after two-electron oxidation of $Zn(L)_2$ (Figure 3) displays a five-line pattern, which was deconvoluted into two subspectra by simulation. The major part of the spectrum, which gives rise to the symmetrical outer four-line pattern [sub-spectrum (b) of Figure 3] is assigned to spin triplet resonances. The sharp central line, which accounts for approximately 20% of the total amount of spin is attributed to $[Zn(L)(L^{\cdot})]^+$. This indicates that the doubly oxidized species is a diradical in which the spins are magnetically coupled (intramolecular spin dipolar coupling). An additional signal could be observed at g ≈ 4.3 both in the perpendicular (Figure 3, inset) and the parallel modes. It corresponds to the forbidden ΔM_S = 2 transition, as expected for an S = 1 system with weak zero-field splitting (ZFS) parameters. The temperature dependence of the signal reveals an excited state for the spin triplet (see Supporting Information) with J = –2.7 ± 0.3 cm^{-1}. From the simulation of the spectrum, the ZFS parameters $|D|$ = 0.0118 cm^{-1} and E/D = 0 could be obtained. DFT calculations were performed in order to obtain insight on the electronic structure of $[Zn(L^{\cdot})_2]^{2+}$. Prior to this analysis, the structural changes resulting from diradical formation have to be commented: A significant elongation of the Zn–O and Zn–N_{linker} bonds [by ca. 0.05 and 0.03 Å, respectively with respect to $Zn(L)_2$] is observed in $[Zn(L^{\cdot})_2]^{2+}$, whereas the Zn–$N_{quinoline}$ bonds are shortened by approximately 0.07 Å. These changes in the bond lengths are two times more pronounced than those observed for the oxidation of $Zn(L)_2$ to $[Zn(L)(L^{\cdot})]^+$. They are also quite similar to those reported for the oxidation of $[Zn(L_{SB})_2]$ to $[Zn(L_{SB}^{\cdot})_2]^{2+}$. Positive spin populations are found at the O1 (0.19), C2 (0.14), C4 (0.23), C6 (0.14), and O2 (0.12) (phenoxyl ring) atoms, as well as, to a lesser extent, at the N1 (0.15), C12 (0.04), and C14 (0.04) atoms (Figure 2). When comparing these contributions to those in $(HL^{\cdot})^+$, one can conclude that coordination of the zinc ion favors localization of the spin density on the phenoxyl ring. Not surprisingly, all pairs of SOMOs are π-orbitals that are mainly distributed over the two phenoxyl ligands (see Supporting Information). The calculated exchange coupling J is –2.73 cm^{-1}, which is in very good agreement with the EPR data. The spatial overlap between the two magnetic pairs of ligand–ligand spin vectors is 0.041. The two radicals are thus weakly antiferromagnetically coupled, giving rise to a spin singlet (S = 0) ground state. The calculated ZFS parameters of the triplet state are D = –0.0098 cm^{-1} and E/D = 0.014 for $[Zn(L^{\cdot})_2]^{2+}$, which is in fairly good agreement with experimental data. The decrease in D when $[Zn(L^{\cdot})_2]^{2+}$ is compared to $[Zn(L_{SB}^{\cdot})_2]^{2+}$ is likely related to the extra delocalization of the spin density promoted by the azo linker {80% of the spin density is located on the phenoxyl moiety in $[Zn(L^{\cdot})_2]^{2+}$ vs. 87% for $[Zn(L_{SB}^{\cdot})_2]^{2+}$}. This spin redistribution may contribute to the lower stability of α-azophenoxyl radicals. It is noteworthy that the system is nearly axial in both cases (the E/D ratio close to zero).

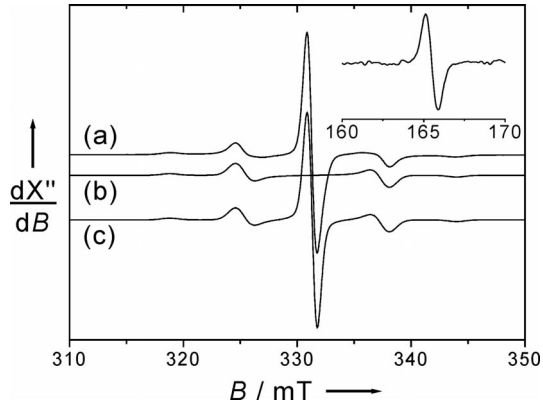

Figure 3. X-band EPR spectra of a 1 mM CH_2Cl_2 solution of the electrogenerated $[Zn(L^{\cdot})_2]^{2+}$: (a) experimental spectrum, (b) simulation of the spin triplet resonances by using parameters given in the text, (c) simulation of the total spectrum by considering 20% of $[Zn(L_{SB})(L_{SB}^{\cdot})]^+$. Inset: low-field region showing the ΔM_S = 2 transition. Freq.: 9.30 GHz, power: 5 mW, mod. freq. 100 kHz, amp.: 0.039 mT. T = 100 K.

Conclusions

Herein we report our first results on the redox chemistry of an α-azophenol ligand, namely HL. The presence of a nitrogen atom α to the hydroxyl group provides the opportunity to form not only "classical" phenoxyl, but also hydrazyl or iminosemiquinonate radical species by one-electron oxidation/reduction. This versatility in the nature of the radical species is remarkable and contrasts sharply with what is commonly observed for Schiff bases. The $Zn(L)_2$ complex is easier to oxidize than the free ligand, affording mono and bis(phenoxyl) radical species. By EPR and UV/Vis spectroscopic analysis, we show that the azo group con-

tributes to an enhanced delocalization of the spin density. It is noteworthy that HL is derived from "naphthol blue" dyes that are widely used in the textile industry and removed by chemical oxidation.[10] We report here direct evidence for the involvement of radicals in the redox activity of closely related compounds.

Experimental Section

Crystal Data

HL: M_w = 670.81, monoclinic, space group C2/*m*, *a* = 24.90(4) Å, *b* = 6.60(2) Å, *c* = 22.20(7) Å, α = 90°, β = 107.3(1)°, γ = 90°, *V* = 3483(14) Å^3, *Z* = 4, D_c = 1.279 g cm^{-3}, *T* = 200 K, μ(Mo-K_α) = 0.84 cm^{-1}. 17803 reflections were collected and corrected for Lorentz and polarization effects. Of 3243 unique reflections (R_{int} = 0.12644), 1769 were observed [$F \geq 2\sigma(F)$] and used in the full-matrix least-squares refinement. *R* = 0.0584, R_w = 0.0767, goodness of fit *S* = 1.36, max./min. residual peaks were 0.29/–0.34 e Å^3.

[Zn(L)$_2$]: M_w = 734.17, monoclinic, space group *P*21/*n*, *a* = 10.449(2) Å, *b* = 25.33(1) Å, *c* = 14.085(5) Å, α = 90°, β = 103.28(2)°, γ = 90°, *V* = 3628(2) Å^3, *Z* = 4, D_c = 1.344 g cm^{-3}, *T* = 200 K, μ(Mo-K_α) = 7.27 cm^{-1}. 15074 reflections were collected and corrected for Lorentz and polarization effects. Of 5994 unique reflections (R_{int} = 0.13606), 4505 were observed [$F \geq 2\sigma(F)$] and used in the full-matrix least-squares refinement. *R* = 0.0632, R_w = 0.0925, goodness of fit *S* = 1.732, max./min. residual peaks were 0.89/–1.72 e Å^3.

CCDC-786219 and -786220 {for [Zn(L)$_2$] and HL, respectively} contain the supplementary crystallographic data for this paper. These data can be obtained free of charge from The Cambridge Crystallographic Data Centre via www.ccdc.cam.ac.uk/data_request/cif.

Supporting Information (see footnote on the first page of this article): UV/Vis and EPR spectra, CV curves, localized SOMOs for [Zn(L)(L$^{\cdot}$)]$^+$ and [Zn(L$^{\cdot}$)$_2$]$^{2+}$, detailed calculated spin density and metrical parameters for the radicals, experimental methods, computational details.

[1] J. Stubbe, W. A. Van Der Donk, *Chem. Rev.* **1998**, *98*, 705.

[2] M. J. McPherson, M. R. Parsons, R. K. Spooner, C. M. Wilmot in *Handbook for Metalloproteins* (Eds.: A. Messerschmidt, R. Huber, T. Poulos, K. Wieghardt), John Wiley and Sons, Chichester, **2001**, vol. 2, pp. 1272; J. W. Whittaker, *Chem. Rev.* **2003**, *103*, 2347.

[3] P. Chaudhuri, K. Wieghardt, *Prog. Inorg. Chem.* **2001**, *50*, 151; F. Thomas, *Eur. J. Inorg. Chem.* **2007**, 2379; F. Thomas in *Stable Radicals: Fundamentals and Applied Aspects of Odd-Electron Compounds* (Eds.: R. Hicks), John Wiley and Sons, Chichester, **2010**, pp. 281.

[4] For recent articles see: T. Storr, E. C. Wasinger, R. C. Pratt, T. D. P. Stack, *Angew. Chem. Int. Ed.* **2007**, *46*, 5198; *Angew. Chem.* **2007**, *119*, 5290; O. Rotthaus, O. Jarjayes, C. Perez Del Valle, C. Philouze, F. Thomas, *Chem. Commun.* **2007**, 4462; T. Storr, P. Verma, R. C. Pratt, E. C. Wasinger, Y. Shimazaki, T. D. P. Stack, *J. Am. Chem. Soc.* **2008**, *130*, 15448; O. Rotthaus, O. Jarjayes, C. Philouze, C. Pérez Del Valle, F. Thomas, *Dalton Trans.* **2009**, 1792; Y. Shimazaki, T. D. P. Stack, T. Storr, *Inorg. Chem.* **2009**, *48*, 8383; M. Orio, O. Jarjayes, H. Kanso, C. Philouze, F. Neese, F. Thomas, *Angew. Chem. Int. Ed.* **2010**, *49*, 4989.

[5] J. Xiang, Y.-G. Yin, P. Mei, Q. Li, *Inorg. Chem. Commun.* **2007**, *10*, 610.

[6] O. Rotthaus, V. Labet, C. Philouze, O. Jarjayes, F. Thomas, *Eur. J. Inorg. Chem.* **2008**, 4215.

[7] M. Orio, C. Philouze, O. Jarjayes, F. Neese, F. Thomas, *Inorg. Chem.* **2010**, *49*, 646.

[8] C. Imbert, H. P. Hratchian, M. Lanznaster, M. J. Heeg, L. M. Hryhorczuk, B. R. McGarvey, H. B. Schlegel, C. N. Verani, *Inorg. Chem.* **2005**, *44*, 7414.

[9] UV/Vis data in CH_2Cl_2 (λ/nm [ε/M^{-1} cm^{-1}]): HL: 363 [11 600], 535 [11 750]; Zn(L)$_2$: 374 [19 500], and 582 [25 980] (the redshift of the bands of Zn(L)$_2$ confirms deprotonation of the ligand); [Zn(L)(L$^{\cdot}$)]$^+$: 350 (sh) [19320], 372 [22280], 426 (sh) [9300], 520 (sh) [15350], 565 (sh) [22000], 606 [22400]; [Zn(L$^{\cdot}$)$_2$]$^{2+}$: 350 (sh) [17930], 368 [18300], 425 (sh) [8130], 520 (sh) [11420], 565 (sh) [12940], 606 [15150].

[10] Y. Yagi, *Bull. Chem. Soc. Jpn.* **1963**, *36*, 487; J. Oakes, P. Gratton, R. Clark, I. J. Wilkes, *J. Chem. Soc. Perkin Trans. 2* **1998**, 2569; K. K. Sharma, B. S. M. Rao, H. Mohan, J. P. Mittal, J. Oakes, P. O'Neill, *J. Phys. Chem. A* **2002**, *106*, 2915.

[11] E. Evangelio, J. Saiz-Poseu, D. Maspoch, K. Wurst, F. Busque, D. Ruiz-Molina, *Eur. J. Inorg. Chem.* **2008**, 2278.

[12] FTIR spectroscopy was found to be uninformative for assigning this predominant tautomeric "NH" form in the solid state. Indeed, the vibration at approximately 1600 cm^{-1}, which is assigned to the asymmetrical N=N stretching mode, overlaps with strong C=C vibrations.

Received: September 23, 2010
Published Online: November 24, 2010

